

# A numerical modelling study of storm surges in Bass Strait

**Kathleen L. McInnes**

CSIRO Atmospheric Research, Aspendale, Australia

and

**Graeme D. Hubbert**

Global Environmental Modelling Systems, Warrandyte, Australia

(Manuscript received March 2002; revised March 2003)

The relationship between severe weather events and storm surges in Bass Strait is investigated. The sustained westerly or southwesterly winds that accompany cold fronts along the south coast are found to be the most common cause of storm surges, although the intensification of low pressure systems in Bass Strait can also produce surges in this region. Two events, caused by cold fronts, are modelled using a high-resolution coastal ocean model. The storm surges produced by meteorological forcing show close agreement with observations at stations west of Bass Strait. In Bass Strait, measured sea-level residuals during strong westerly wind events exhibit a semi-diurnal oscillation resulting from an approximate 20 minute delay between the measured high tides and the predicted tides used to extract the sea-level residuals. This delay can be reproduced by the model when run with atmospheric and tidal forcing and the tides subsequently removed, indicating that the enhanced westerly current during the surge event interacts with the tidal currents to produce a temporary phase delay in the tides in western Bass Strait, although the physical mechanism behind the response is not clear. The contribution to storm surge height due to atmospheric pressure is found to be only around 10 per cent of the inverse barometer effect indicating that wind stress is by far the dominant component of the storm surge height in this region. The role of remote and local wind forcing in Bass Strait is investigated by performing model simulations where the western boundary of the model domain is moved progressively eastwards. Exclusion of the narrow shelf region immediately to the west of Bass Strait reduces the peak surge within Bass Strait by between 50 and 80 per cent in broad agreement with theoretical studies. An investigation of the effect of wind speed changes on storm surge height reveals that storm surge height responds linearly to changes in wind strength with a proportionality coefficient of around two.

## Introduction

Storm surges are temporary elevations or depressions in sea-surface height driven by surface winds and changes in atmospheric pressure. Their severity

depends on the strength and duration of the atmospheric disturbance, and the structure of the coastal terrain. Severe storm surges can cause inundation of low-lying coastal plains and flooding of river systems and, combined with wind-generated wave action, can cause coastal and estuarine erosion.

---

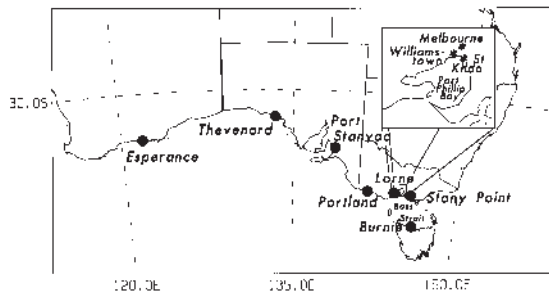
*Corresponding author address:* Dr Kathleen McInnes, CSIRO Atmospheric Research, Private Bag No. 1, Aspendale, Vic. 3195, Australia.

Email: kathleen.mcinnes@csiro.au

Much of Australia's south coast features a relatively wide shallow continental shelf. Combined with the frequent passage of mid-latitude depressions and cold fronts, this coastline is a favourable region for the generation of storm surges. The coastal configuration further east is unusual in that the shelf narrows considerably just before the entrance into Bass Strait (Fig. 1) which itself features relatively shallow bathymetry, dropping off steeply at its western and eastern boundaries. This uniquely configured coastline has been the subject of a number of studies that address the nature and propagation characteristics of disturbances generated along the south coast by wind stresses.

Of particular interest and considerable debate has been how such disturbances are modified when they reach the western boundary of Bass Strait. As noted by Provis and Radok (1979), the typical travel times for eastward propagating coastally trapped disturbances along the south coast are similar to those of the weather systems that traverse the coast. The relative roles of the local and upstream wind forcing, on disturbances in Bass Strait has undergone considerable debate in the literature. Church and Freeland (1987) suggest that, at the more energetic frequencies, most of the wind-forced coastal-trapped wave (CTW) energy generated along the south coast travels through Bass Strait to the east coast of Australia. On the other hand, Clarke (1987) proposes that most of the wave energy reaching the east coast is generated within Bass Strait by the stronger wind stresses that occur there. However, Baines et al. (1991) show that the analysis of Clarke (1987) is incorrect because his analysis omits the transmitted shallow-water Kelvin wave component due to erroneous assumptions, and this leads to solutions that do not conserve mass. Middleton (1988) presents solutions for the shelf response to an oscillatory coastal flux through a strait and shows that CTWs off the east coast would be generated and coherent with the currents within Bass Strait. Morrow et al. (1990) show that winds and currents in eastern Bass Strait are in phase and highly coherent, unlike those measured on the east coast, implying that much of the energy flux reaching the east coast must be generated within Bass Strait. Baines et al. (1991) apply a forced Kelvin-wave model to observational data to infer that approximately two-thirds of the flux through Bass Strait is due to forcing to the west and the remaining one-third due to forcing within Bass Strait. A study by Middleton and Viera (1991), in which analytical models for local wind driven Kelvin waves and remotely forced CTWs to the west of Bass Strait are developed, confirms this result for low frequency (ten day) oscillations. Implicit in these models and the improved energy conserving solutions presented in Middleton (1991) is

**Fig. 1** Locations of the sea-level monitoring stations. Inset shows an enlargement of Port Phillip Bay with relevant place names indicated.



a mechanism by which Continental Shelf Waves (CSW) and CTW energy can be scattered into and out of Bass Strait.

Numerical modelling of storm surges along Australia's south coast commenced with Fandry (1982) in which a depth-averaged, shallow-water equation model with idealised bathymetry was used to simulate the effects of various wind stress configurations on the flow in Bass Strait. Subsequently, Fandry et al. (1985) developed a numerical model to describe the tidal regime of Bass Strait. Hubbert et al. (1990) developed a storm surge model that utilises realistic bathymetry and spatially varying winds and pressure from atmospheric analyses or forecast models. Currents and sea levels in Bass Strait were simulated to test the model performance and found to show close agreement with observations. Middleton and Black (1994) use a numerical model to verify the behaviour of CSWs as they encounter the western entrance to Bass Strait. Results are consistent with analytical solutions derived in Middleton and Viera (1991) and indicate that about 50 per cent of CSW energy incident at the western entrance is scattered into Bass Strait. The circulation driven by a 10 cm amplitude incident CSW was similar to that driven by a 0.1 Pascal zonal wind stress.

In the present study, the storm surge model described in Hubbert et al. (1990) and Hubbert and McInnes (1999) is used to simulate two storm surges in Bass Strait. The aim of the study is to see how well the model can reproduce the sea levels associated with these storm events as well as examine whether the model results can reproduce those determined from analytical studies. The model is also used to explore aspects of the storm surges including the relative roles of wind stress and atmospheric pressure forcing, the interaction of the storm surge with tides, the effect of changes in the computational domain on

the solution and the relationship between wind strength and storm surge height. The paper is organised as follows; a brief climatology is presented of storm-surge events in Bass Strait and a description of the synoptic situations responsible for their generation; the storm-surge model is then described and results from two numerically simulated storm surges and a range of sensitivity experiments are presented and discussed. Finally, a summary and conclusions are presented.

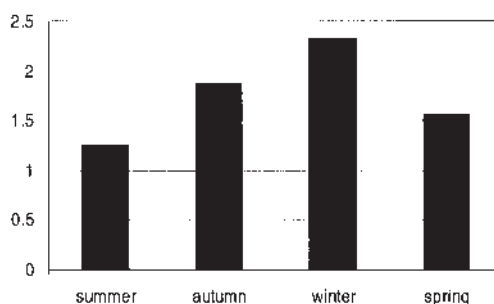
## Synoptic overview

Episodes of elevated sea level in Bass Strait have been examined in eight years of data collected from tide gauges established by the National Tidal Facility in 1993. Sea-level residual data, in which the re-predicted tidal component is subtracted out to leave the sea-level response due to meteorology only, is used to identify incidences where sea levels exceed 0.5 m at either Lorne or Stony Point (see Fig. 1 for locations). A total of 43 events occurred over the eight-year period and their seasonal frequencies are represented in Fig. 2. These data show that elevated sea-level events occur in all seasons, although they tend to be slightly more frequent in autumn and winter. The prevailing meteorological conditions in the majority (approximately 83 per cent) of cases are cold fronts that traverse the south coast. Less commonly, they are caused by mesoscale low pressure systems which develop and intensify within Bass Strait.

Cold fronts affect the southern coastline all year round although the winter months, when the subtropical ridge has moved northwards over the continent, are more likely to yield conditions that are conducive to storm surge generation. At this time, the southern coastal regions tend to be under the influence of more sustained westerly winds. In summer on the other hand, cold fronts along the southern coastline are often the shallow, northern extents of deeper frontal systems which pass well to the south of the continent (Reeder et al. 1991 and McInnes et al. 1994). These fronts are often located between two ridges of high pressure which bring lighter winds to the coastal regions, and so the incidence of intense and prolonged postfrontal westerly or southwesterly winds, capable of producing surges, is less common.

The second and less common cause of storm surges in Bass Strait is mesoscale lows. Of the events identified in the present study, the majority occurred in spring and summer. While less common, it is noteworthy that the worst storm surge event to occur in Bass Strait in the twentieth century was produced by such a system in November 1934. The combination of the low pressure and the southerly and southwest-

**Fig. 2** Frequency histogram showing the seasonal incidence of elevated sea levels of 0.5 m or greater at Lorne or Stony Point, based on NTF data from June 1993 to May 2001.



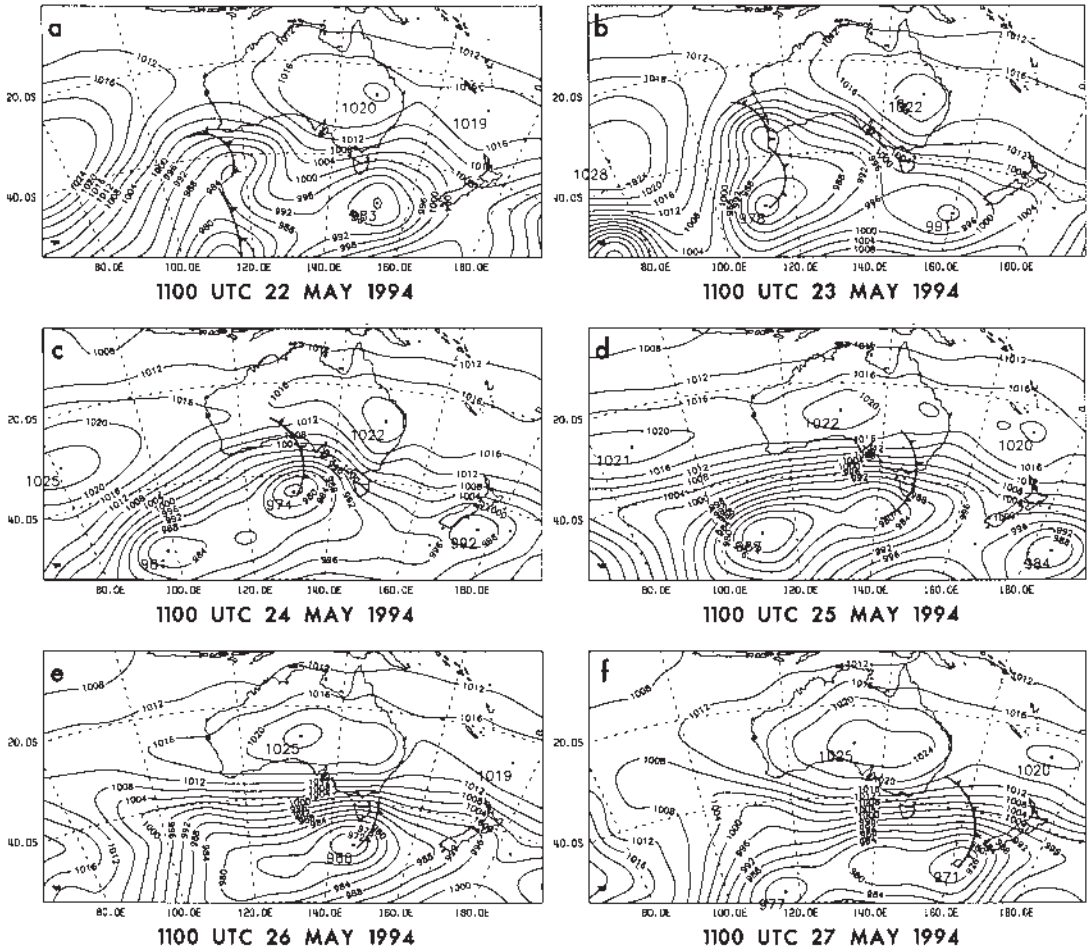
erly gales occurring on the western side of the depression produced a storm surge which peaked at 1.33 m above mean sea-level at Williamstown (see inset of Fig. 1) (Adams 1987). Of significance also, was the intense rainfall that accompanied this low and produced the worst floods experienced in this region in recorded history. About 144 mm of rain fell in Melbourne over a 30-hour period, coinciding with the peak surge and leading to massive flooding in low-lying coastal areas. Storms of such intensity have not occurred in recent years, and therefore will not be modelled in the present study. The sea-level response of similar systems on the east coast of Australia, has been modelled by McInnes and Hubbert (2001).

The first of two cold fronts to be investigated in this study occurred in May 1994 and produced elevated sea levels along the entire south coast. The sea-level pressure associated with this event is shown in Fig. 3. A ridge of high pressure is situated over the continent and a low pressure system and associated cold front is located to the southwest of the continent. As the front moves eastwards over the following five days, the post-frontal winds have a largely coast-parallel component at all times. The onshore Ekman transport driven by the winds raises coastal sea levels which through geostrophic adjustment produces an alongshore current.

The sea-level pressure for the second cold front to be modelled is shown in Fig. 4. A storm surge resulting from this front occurred in Bass Strait on 6 and 7 November 1994. A ridge of high pressure was located over the west of the continent and a low and cold front moved up from the southwest bringing severe winds to the south-eastern coastal regions.

The sea-level residuals for May 1994 are presented in Fig. 5(a) and show that elevated sea levels com-

**Fig. 3** Bureau of Meteorology analyses of mean sea-level pressure for the May storm-surge event.



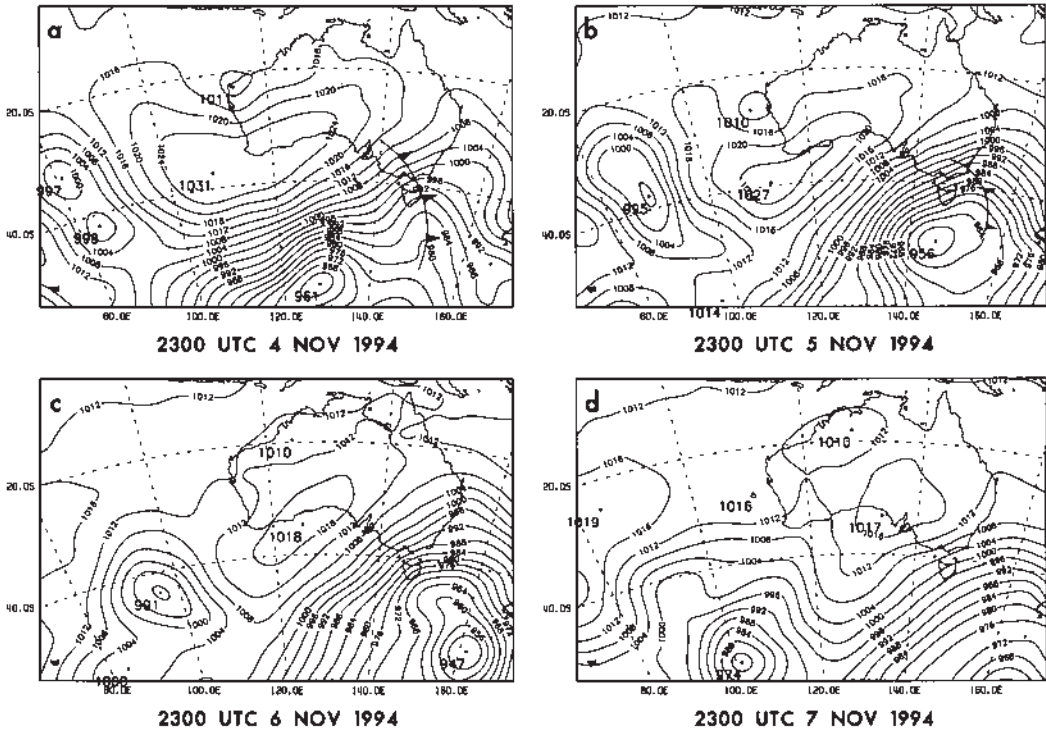
mence in the west on 22 May and move progressively east as the front moves east. Peak sea levels occur in Bass Strait on 26 May, during which time the low is to the south of Tasmania, and a strong north-south pressure gradient is situated over Bass Strait (Fig. 3(e)), producing gale-force westerly winds. Three less significant events also occurred earlier in May and were caused by cold fronts that mainly affected the eastern half of the south coast. The sea-level residuals for November (Fig. 5(b)) show that the storm surge occurred at tide gauges east of Thevenard and reached a metre in height at Stony Point.

An oscillation can be seen in the residual sea-level signal at the three Bass Strait tide gauges of Lorne, Stony Point and Burnie. The period is approximately 12 hours and the signal is more or less in phase on both sides of Bass Strait and about 180° out of phase

with the tides. Examination of NTF sea-level data and the predicted tides from which the residuals are calculated reveals a phase delay between the times of the high tides in the two datasets with the high tides in the observed data occurring about 20 to 30 minutes later than in the predicted tides. This feature will be investigated further in a later section.

Rainfall generally accompanies cold fronts, particularly during the winter months, however it is not usually intense. For example, for the May and November cases, the maximum daily rainfall totals near Lorne were about 20 and 12 mm respectively and near Stony Point, they were 18 and 29 mm respectively. The risk of severe flooding due to the combination of storm surge and rainfall run-off during the passage of fronts is therefore fairly low. However, it is worth noting that in both cases studied here, minor flooding occurred in

Fig. 4 Bureau of Meteorology analyses of mean sea level pressure for the November storm-surge event.



low-lying coastal suburbs of Melbourne. High resolution modelling of the flooding caused by the combination of tide and storm surge during these two events at two low-lying coastal locations in Melbourne was undertaken in Hubbert and McInnes (1999).

**The model and atmospheric forcing**

The storm surge model used in this study is a depth-integrated, ocean-current model developed specifically to simulate currents and sea-surface elevations on continental shelves. An earlier version of the model is described in Hubbert et al. (1990) and more recent changes are documented in Hubbert and McInnes (1999). For completeness, a brief description of the most relevant features of the model is given here.

The shallow-water equations are solved on an Arakawa C-grid using a time-splitting finite difference scheme. Three different time steps are used to solve the gravity wave, advective and physics components of the equations of motion. On the lateral boundaries, a radiation condition that solves for the

group velocity is used. The surface wind stresses are computed using a quadratic relationship in which the drag coefficient is based on Smith and Banke (1975), and the bottom stress is represented by a depth-dependent quadratic friction relationship, which follows Signell and Butman (1992).

At the lateral boundaries of the model, a boundary condition on perturbation height,  $\zeta$ , is imposed, i.e.

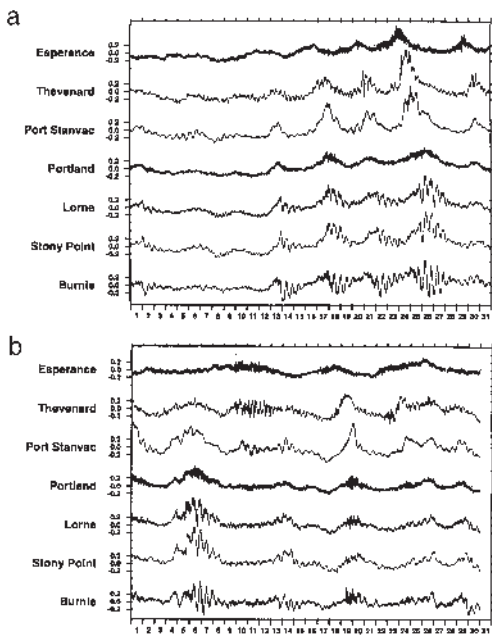
$$\zeta = \zeta^T + \zeta^M \quad \dots 1$$

where  $\zeta^T$  is the perturbation height due to tidal variations and  $\zeta^M$  is the elevation due to the inverse barometer effect and is equal to

$$(P_0 - P_a) / \rho_w g \quad \dots 2$$

where  $P_0$  is taken to be a standard atmosphere pressure of 1013.25 hPa,  $P_a$  is the atmospheric pressure,  $\rho_w$  is water density and  $g$  is the acceleration due to gravity. Tidal constituents (tidal phases and amplitudes) were included for seven leading tidal constituents; the principal lunar and solar semidiurnal

**Fig. 5 Residual sea-level heights produced by the National Tidal Facility for (a) May 1994 and (b) November 1994, at the stations indicated in Fig. 1.**



constituents, M2 and S2; the principal lunar diurnal constituent, O1; the lunar elliptic diurnal and semidiurnal constituents, Q1 and N2; and the lunisolar diurnal and semidiurnal constituents, K1 and K2. These constituents were obtained from a 30-minute global tidal model which models tidal currents and assimilates satellite measurements of ocean surface heights from the TOPEX/POSEIDON altimeters (Le Provost et al. 1995). The tides are applied as an amplitude change in water levels on the lateral boundaries of the model grid (McInnes et al. 2002). For the normal component of current, a radiation boundary condition following Miller and Thorpe (1981) is applied to the outflow velocities to prevent the build up of wave energy within the numerical domain, while on inflow boundaries, a zero-gradient condition is applied.

High resolution winds and surface pressure, needed to drive the storm surge model, were obtained by running a limited area atmospheric model based on McInnes and Hess (1992) at 25 km horizontal resolution over a region extending from 125°E to 153°E and 27°S to 45°S. Fifteen vertical levels were used with the lowest model level located at approximately 10 m above the surface. The atmospheric analyses used to initialise and provide

boundary conditions for this model were obtained from 12-hourly Australian Bureau of Meteorology regional analyses (Mills and Seaman 1990). Output from the atmospheric model was stored every six hours. Surface pressure and 10 m winds were then interpolated spatially to the storm surge model grid to provide the surface boundary conditions.

A comparison of the lowest model level winds is made with observed winds at Thevenard and St Kilda for the May event (Fig. 6). At St Kilda, the wind observations were lower than the 10 m level used by the model and so they were adjusted using the logarithmic wind law assuming neutral conditions and a roughness length of 3 cm. The assumption of neutrality is reasonable in high wind conditions. In general, the model has captured the overall variation in wind, particularly in relation to the timing of the peak wind strength. However, the model has systematically over-estimated the wind speed at both locations. Errors in wind speed will lead to an approximate doubling in the errors in wind stress.

## Storm surge model results

The May and November storm-surge events are modelled on a 5 km resolution grid covering the region shown in Fig. 7. The simulation of the May event is conducted over an eight day interval from 1100 UTC 21 May to 1100 UTC 29 May 1994 while the November storm-surge event is simulated over four days from 2300 UTC 3 November to 2300 UTC 7 November 1994. Both events are modelled with 'meteorology-only' forcing to investigate the ability of the model to reproduce the observed storm-surge signal along the south coast. A 'winds-only' simulation is then performed to investigate the role of the inverse barometer effect on sea levels by removing the contributions from the pressure gradient term in the equations of motion and the lateral boundary condition on perturbation height. Two experiments: a 'tides and meteorology' simulation and a 'tides-only' simulation, are performed to see whether the model also reproduces the phase delay that occurs in sea level residuals at Lorne, Stony Point and Burnie when westerly winds are present. The purpose of this set of simulations is to see whether the model can be used to investigate this phenomenon in a subsequent study. Experiments are then performed for the May event in which the western boundary of the model is moved progressively eastwards to investigate the impact of local and remote wind forcing on the amplitude of the storm surge in Bass Strait. Finally the effect of wind speed changes on the storm-surge height is investigated.

Fig. 6 Modelled (heavy lines) and observed (thin lines) wind speed and direction for (a) Thevenard, and (b) St Kilda for the May storm-surge event. The time series commences at 1100 UTC 21 May 1994.

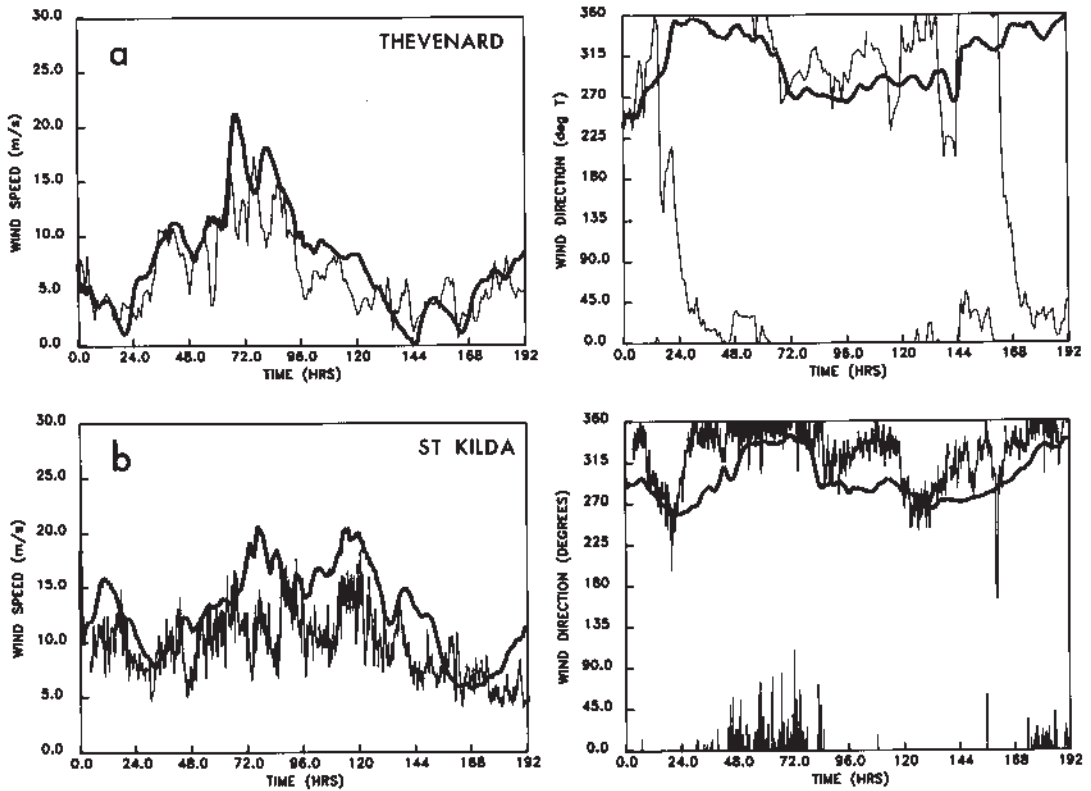
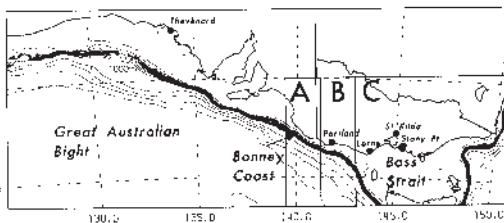


Fig. 7 Region over which the storm surge model is run. Bathymetric contours are shown in intervals of 100 m up to 1000 m and then in 1000 m increments thereafter.



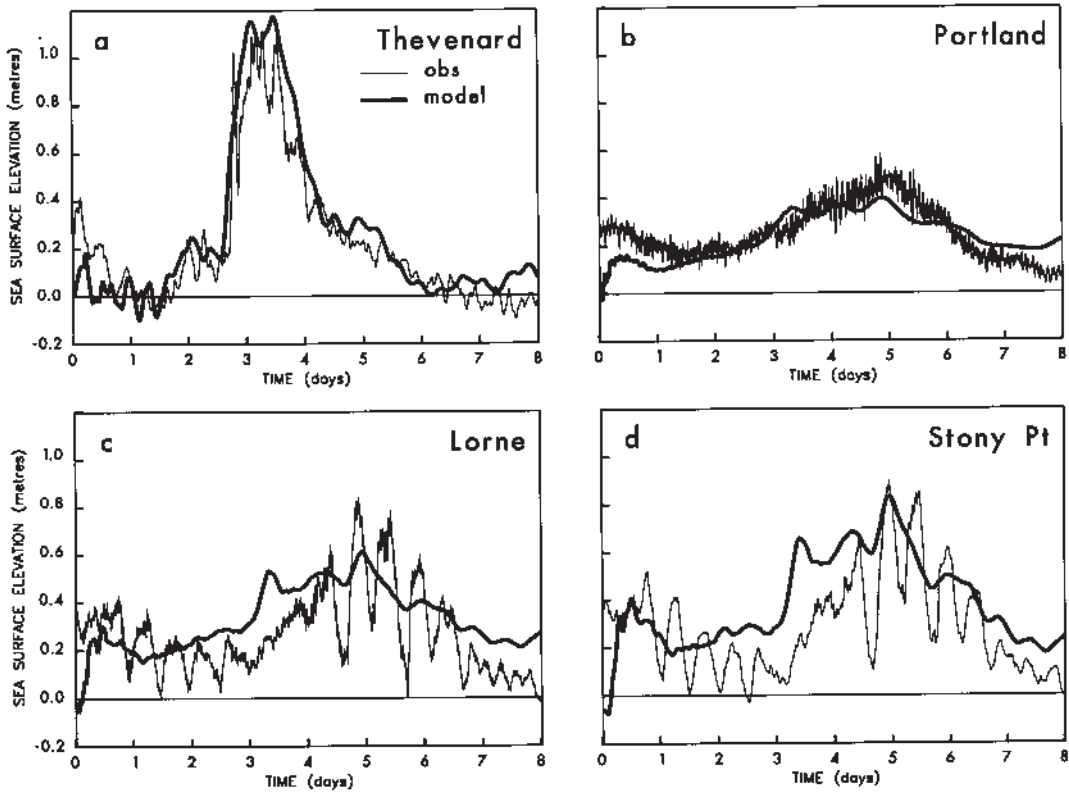
**‘Meteorology-only’ simulations**

Time series of observed and modelled sea level heights for the May storm-surge event at four locations are shown in Fig. 8. At Thevenard, the observed sea levels reach peak heights of around 1.1 m just over 3 days into the model simulation. The

modelled surge shows remarkably close agreement with the observed surge in terms of timing, although the peak is slightly overestimated. At Portland however, observations indicate a lower peak surge of around 0.5 m, which is underestimated by the model. The time series of observed sea levels at Lorne and Stony Point exhibit oscillatory signals with a 12-hour period superimposed on the background residual heights. While the oscillations are not present in the modelled elevations at Lorne and Stony Point, there is good agreement in the overall timing of the elevated sea levels. The oscillation in the residual signal will be investigated subsequently.

Figure 9(a) shows the wind generated current at 72 hours into the simulation which is the time of the peak storm surge at Thevenard. At this time, an eastward flowing current confined to the shallow continental shelf has become established. The simulated sea-surface elevations are shown in Fig. 9(b) and indicate a pronounced build-up of water in the vicinity of Thevenard and some increase in elevations commencing

Fig. 8 Observed and modelled residual sea-level height for the May storm surge event at (a) Thevenard, (b) Portland, (c) Lorne and (d) Stony Point. Time series commences at 1100 UTC 21 May 1994.



ing in Bass Strait. By 120 hours, the storm surge is reaching its maximum height in Bass Strait. Currents at this time are shown in Fig. 9(c). Verification data for the currents were not available, however, the spatial pattern of the flow in Bass Strait is similar to that obtained in Hubbert et al (1990) during a similar but weaker westerly wind event, for which comparisons between modelled and observed currents showed close agreement. An interesting feature to note is the weak southbound current along the western boundary of Bass Strait, which is also reflected in the height contours as a wedge of higher sea levels extending southwards along the shelf break (Fig. 9(d)). This current is associated with the propagation of a CSW, which travels southwards to the west coast of Tasmania on the shelf break, and is balanced on the shallow side of the shelf by a perturbation with Kelvin wave characteristics propagating to the north-east (Baines et al. 1991; Middleton and Viera 1991; Middleton and Black 1994).

The November 1994 observed and modelled storm surges are shown in Fig. 10. Thevenard is located to

the west of the most intense atmospheric forcing in this event and so the observed and modelled sea-level residuals reach only about 0.2 m in height. The modelled sea levels at Portland are again slightly underestimated, while at Lorne and Stony Point, the timing of the surge agrees well with observations if the oscillation in the observed time series is disregarded.

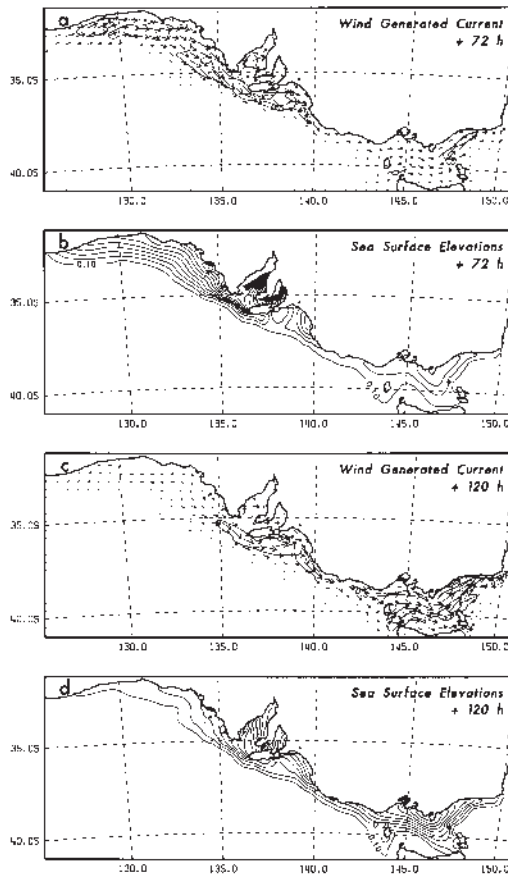
#### 'Wind-only' simulations

Storm surges are attributed to both wind stress and falling atmospheric pressure with the effect of the wind being dominant (Gill 1982, p.340). The component of sea-level change produced by atmospheric pressure changes is often estimated using the static relationship,

$$\Delta\zeta = (P_0 - P_a) / \rho_w g \quad \dots 3$$

– the so-called inverse barometer effect. Implicit in this relationship is the assumption that the ocean has fully adjusted to the changes in atmospheric pressure. This is achieved by the development of down-gradient

**Fig. 9** (a) Wind generated current, (b) sea-surface elevations at 72 hours into the model simulation, (c) wind generated current and (d) sea-surface elevations at 120 hours for the May storm-surge event. Current speed contours are in intervals of  $0.5 \text{ m s}^{-1}$  and height contours are in intervals of  $0.1 \text{ m}$ .



ocean currents which are eventually reduced to zero by frictional processes, yielding an adjusted sea surface that is in balance with the atmospheric pressure. In practice, it is not clear that this balance is achieved on the time scales associated with the occurrence of weather phenomena.

Examination of Figs 3 and 4 indicates that pressure variations are likely to play a greater role in the November case with pressure falling to around 990 hPa along the Victorian coast during the passage of the front compared with the May event in which pressure remained at around 1000 hPa during the period of strongest winds as the front crossed the region.

Storm-surge simulations for both the May and November cases are conducted without the forcing

due to atmospheric pressure leaving only the wind stress to drive the ocean circulation. Table 1 compares actual heights from the model simulations with inverse barometer values. The difference in height obtained from the full 'meteorology' and 'wind only' simulations is typically only about 10 per cent of that expected due to the inverse barometer effect. This leads to an average reduction of around three per cent in storm-surge height over the period 1200 UTC 24 – 27 May when surface pressure forcing is absent. For the November event, the average reduction in height over the period 0000 UTC 5-7 November is eight per cent, six per cent and four per cent for Portland, Lorne and Stony Point respectively. Furthermore, the average wind stress per unit depth in the x-direction, based on an average wind speed of  $20 \text{ m s}^{-1}$ , drag coefficient,  $C_D$ , of 0.002 and average depth of Bass Strait of 80 m is of the order of  $1 \times 10^{-2} \text{ kg m}^{-2} \text{ s}^{-2}$ . In comparison, the x-component of pressure gradient through Bass Strait is of the order of  $1 \times 10^{-5} \text{ kg m}^{-2} \text{ s}^{-2}$  indicating that wind stress is by far the dominant forcing term under these conditions. Clearly the balance that is implied by the inverse barometer rule is not achieved in Bass Strait during the passage of these cold fronts.

#### 'Meteorology and tide' simulations

In this section, the oscillation in the NTF residual data at Lorne, Stony Point and Burnie is investigated using the model. Two model simulations of the May event are performed. In the first, both tidal and wind forcing is applied and so the sea-level variations are analogous to those measured at the tide gauge. The second simulation contains tidal forcing only. The time series from the 'tide-only' simulation at the tide gauge locations are subtracted from those of the 'winds and tide' simulation to produce time series that are analogous to the residuals generated by the NTF.

The results are shown in Fig. 11 for Portland, Lorne, Stony Point and Burnie along with the NTF residuals and the time series from the 'meteorology only' simulation. The most striking aspect of the results is that the model-generated sea levels for Lorne, Stony Point and Burnie (Figs 11 (b)-(d)) exhibit a remarkably similar oscillation to the NTF residuals although the amplitude is somewhat smaller. This indicates that the westerly wind-induced currents interact with the tidal currents to alter the phase of the tides within Bass Strait. The high tides in the 'meteorology and tide' simulation occur on average 20 minutes later at Lorne, Stony Point and Burnie. The same average delay in high tides is present in the NTF data compared to the NTF tidal predictions over the same time interval.

In Bass Strait, tidal behaviour is predominantly semi-diurnal. The westward travelling tidal wave

Fig. 10 Observed and modelled residual sea-level height for the November storm-surge event at (a) Thevenard, (b) Portland, (c) Lorne and (d) Stony Point. Time series commences at 2300 UTC 3 November 1994.

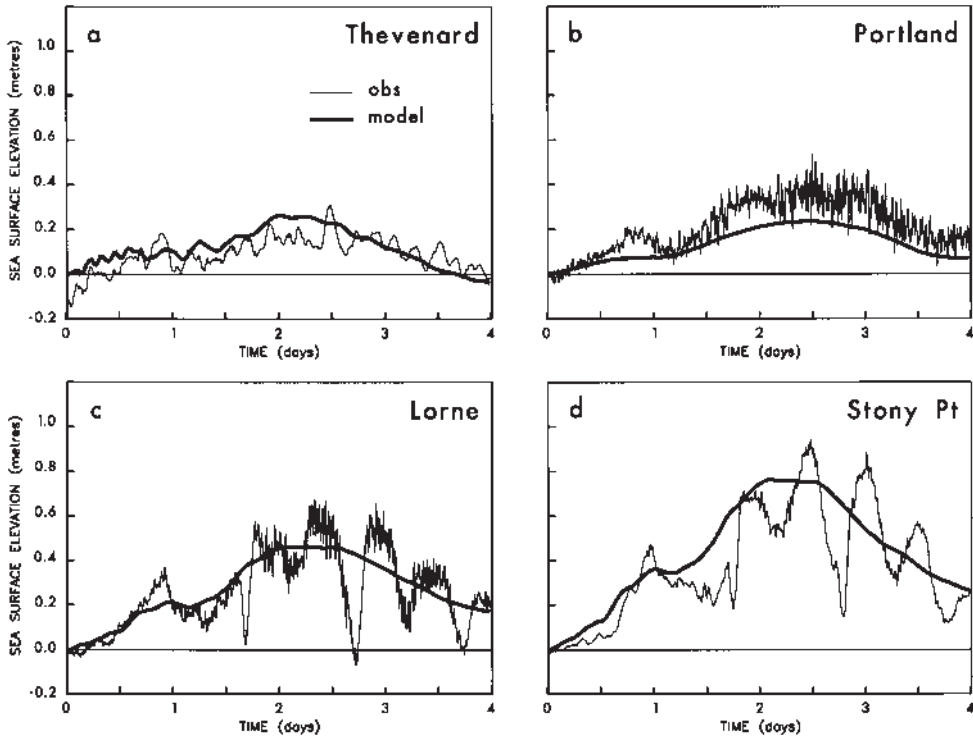
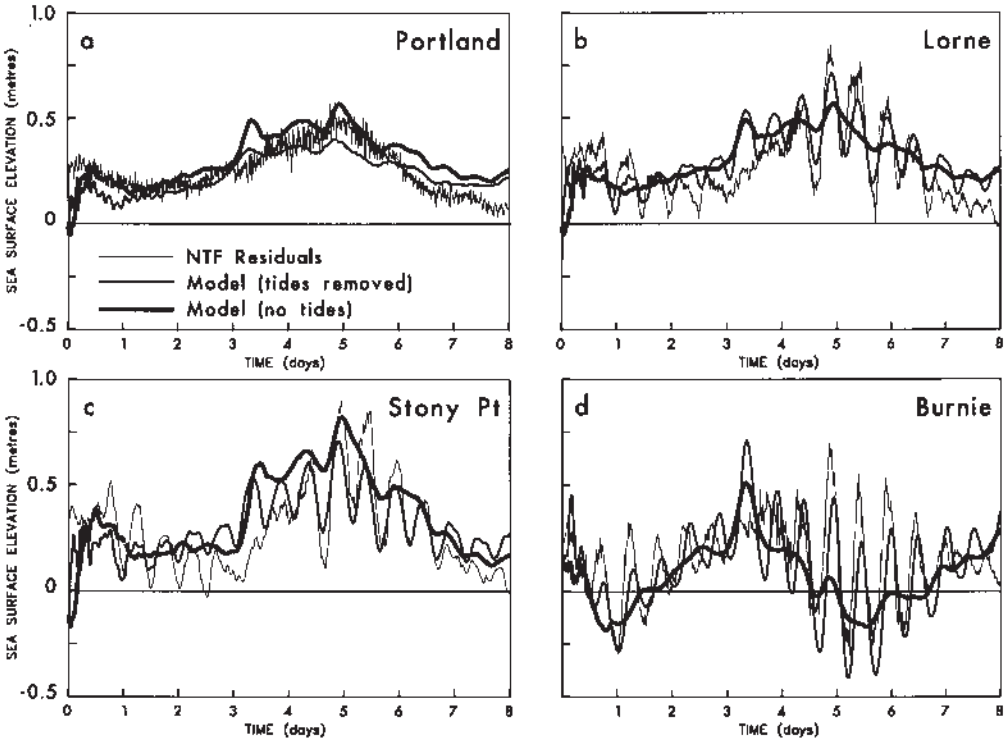


Fig. 11 Comparison of measured residual sea-level height with modelled sea levels from a simulation with only meteorological forcing and a simulation with tidal and meteorological forcing where the tidal component has been subsequently removed for (a) Portland, (b) Lorne, (c) Stony Point and (d) Burnie.



**Table 1.** Atmospheric pressure, the sea-level rise due to the inverse barometer effect as defined by Eqn 3, the modelled sea levels in the Meteorology and Winds Only simulations and the difference in sea level between these two simulations.**Portland**

<i>Date / Time</i>	<i>Atmospheric Pressure (hPa)</i>	<i>Inverse Barometer (cm)</i>	<i>'Meteorology' Simulation (cm)</i>	<i>'Winds only' Simulation (cm)</i>	<i>'Meteorology' – 'Winds only' (cm)</i>
0000 UTC 5 Nov	1006	7	11.7	10.6	1.1
0000 UTC 6 Nov	994	19	29.7	27.3	2.4
0000 UTC 7 Nov	998	15	26.8	25.9	0.9
1200 UTC 24 May	996	17	29.2	28.0	1.2
1200 UTC 25 May	999	14	37.0	36.0	1.0
1200 UTC 26 May	1004	9	37.2	36.2	1.0
1200 UTC 27 May	1014	-1	28.1	27.9	0.2

**Lorne**

<i>Date / Time</i>	<i>Atmospheric Pressure (hPa)</i>	<i>Inverse Barometer (cm)</i>	<i>'Meteorology' Simulation (cm)</i>	<i>'Winds only' Simulation (cm)</i>	<i>'Meteorology' – 'Winds only' (cm)</i>
0000 UTC 5 Nov	1001	14	22.3	21.1	1.2
0000 UTC 6 Nov	990	23	50.4	47.4	3.0
0000 UTC 7 Nov	993	20	38.7	36.6	2.1
1200 UTC 24 May	1000	13	50.3	49.4	0.9
1200 UTC 25 May	998	15	57.5	55.6	1.9
1200 UTC 26 May	1002	11	39.7	39.3	0.4
1200 UTC 27 May	1013	0	25.1	25.1	0

**Stony Point**

<i>Date / Time</i>	<i>Atmospheric Pressure (hPa)</i>	<i>Inverse Barometer (cm)</i>	<i>'Meteorology' Simulation (cm)</i>	<i>'Winds only' Simulation (cm)</i>	<i>'Meteorology' – 'Winds only' (cm)</i>
0000 UTC 5 Nov	1000	13	39.4	37.5	1.9
0000 UTC 6 Nov	989	24	82.7	79.6	3.1
0000 UTC 7 Nov	991	22	58.9	56.4	2.5
1200 UTC 24 May	1003	10	65.9	65.2	0.7
1200 UTC 25 May	1000	13	85.0	84.0	1.0
1200 UTC 26 May	1002	11	54.8	54.4	0.4
1200 UTC 27 May	1013	0	30.4	30.2	0.2

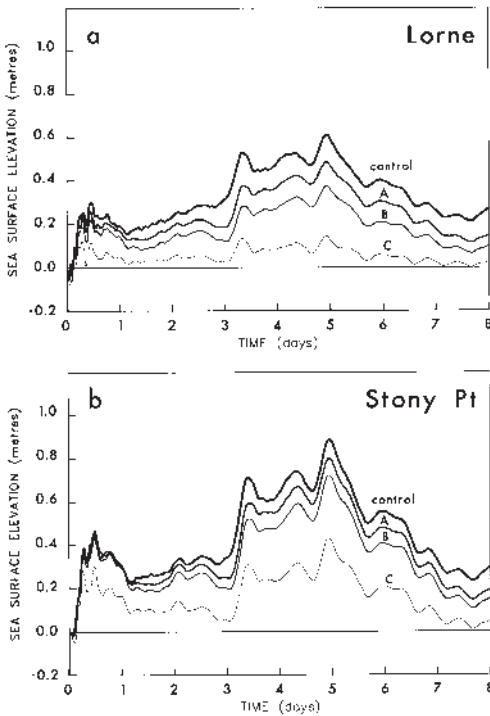
enters Bass Strait not only from the east but also propagates around Tasmania to enter from the west so that much of the region experiences high tides simultaneously (Easton 1970). The simulations suggest that the action of stronger westerly currents during frontal events displaces the convergence zone or node for the tidal currents further eastwards. This results in a delay in the filling of western Bass Strait and hence a delay in the occurrence of high tides at the three tide gauges located there. However the mechanism by which this occurs is not clear. A scale analysis indicates that increased advection is not likely to be the cause of the delay. It is planned to use the model to investigate this phenomenon in more detail in a subsequent study.

**Effect of computational domain changes**

A set of experiments was conducted to examine the sensitivity of the sea level response in Bass Strait to the location of the western boundary of the model to investigate the relative roles of local and remote wind forcing on the storm-surge heights in Bass Strait. The model is run in 'meteorology-only' mode and the regions over which the experiments are run are shown in Fig. 7. Region A has its boundary at the western end of the Bonney Coast, region B just west of Portland, and C at the western edge of Bass Strait. Results from these simulations are shown in Fig. 12.

The storm-surge heights at Lorne and Stony Point in the region A simulation are lower by about 20 to 10 per

**Fig. 12** Comparison of modelled sea-level elevation at (a) Lorne and (b) Stony Point for model simulations carried out over the entire region (control) as well as the subregions A, B and C as shown in Fig. 7.



cent respectively compared to the control run and this reduction is apparent throughout the simulation. Results for region B indicate further reductions in height of approximately 40 per cent and 20 per cent for Lorne and Stony Point respectively. The most dramatic impact on sea-level elevations is seen in results generated over region C. Here, the reductions in peak surges at Lorne and Stony Point are 70 per cent and 50 per cent respectively. These results are consistent with Baines et al. (1991) and Middleton and Viera (1991), who find that the remotely generated CTW contributes to about two thirds of the signal in Bass Strait while local wind forcing makes up the rest. The results also indicate that the location of the western boundary has a stronger influence on sea-level heights at locations in closest proximity than those further east. Furthermore, the results suggest that a computation region spanning much of the south coast is needed to model the full response of Bass Strait to westerly wind events.

**Impact of wind speed changes**

The relationship between wind speed changes and peak storm surge is also investigated. Reductions of

ten per cent and increases of five per cent, ten per cent and twenty per cent are made to the wind fields over the computational domain in both events, which are then used to force the storm-surge model. Atmospheric pressure forcing remains unchanged. The results are summarised in Fig. 13.

The percentage change in peak storm-surge height at a given location varies approximately linearly with percentage change in wind speed. In the May case, the variation in storm-surge height is about twice that of the wind speed variation at Thevenard, Stony Point and Lorne, and between one and 1.5 times greater at Portland. For the November case however, the storm-surge response at all locations is a little over twice that of the wind speed change. A simple scale analysis shows that this linear relationship is to be expected. Since the east-west current  $u$  is approximately geostrophic over the width,  $W$  of Bass Strait, then

$$u \sim \frac{g}{f} \frac{\Delta \zeta}{W}$$

where  $f$  is the Coriolis parameter and the  $u$ -momentum equation reduces to a balance between surface and bottom stress i.e.  $C_D \rho_a U_a^2 \sim K \rho_w u^2$ , where  $C_D$  is the surface drag coefficient,  $\rho_a$  is the density of air,  $U_a$  is the east-west wind speed,  $K$  is the bottom friction coefficient and  $C_D \sim K$ . Therefore, the change in sea level  $\Delta \zeta$  scales as

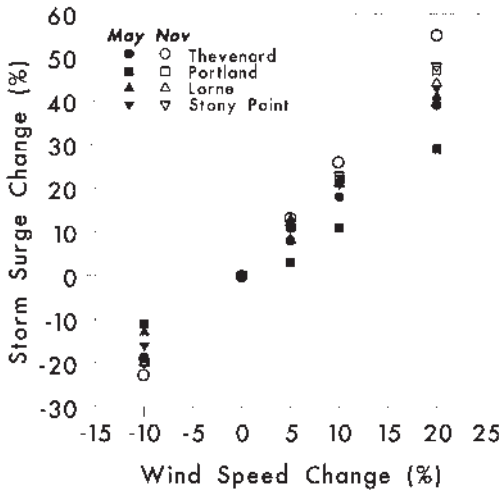
$$\frac{f}{g} W \sqrt{\frac{\rho_a}{\rho_w}} U_a$$

which is, approximately a linear relationship. This linear relationship is consistent with the earlier finding that atmospheric pressure forcing is not significant in these events. The clear implication from this set of experiments is that any long-term change in wind climate along the south coast, which results in the more frequent occurrence of stronger cold fronts, could dramatically increase the incidence of severe storm-surge events.

**Summary and conclusions**

In this study, two storm-surge events in Bass Strait have been investigated using a numerical coastal ocean model. Examination of eight years of sea-level data in Bass Strait indicates that storm surges occur year round, although they are more common in winter. About 83 per cent of the events that occurred over this period were caused by the predominantly westerly winds associated with cold fronts. The remaining storm-surge events were caused by intense mesoscale low pressure systems which either developed or intensified in Bass Strait. While less common, they

**Fig. 13** Percentage storm surge change as a function of the percentage change in wind speed, at each of the four stations based on sensitivity experiments.



are potentially more damaging because of the intense rainfall that can accompany them and which, combined with the storm surge, can produce severe coastal flooding. Indeed, one such event, which occurred in early November 1934, was responsible for the highest storm surge and worst flooding over Melbourne in recorded history.

Two storm-surge events caused by cold fronts were modelled using a high resolution storm-surge model forced by realistic wind and pressure fields. Close agreement was found between the observed and modelled surge at locations to the west of Bass Strait when only atmospheric forcing was applied to the storm-surge model. However, within Bass Strait, the timing of the surge was in general agreement but the model simulation lacked an oscillatory feature that was present in the sea level residuals and which resulted from a phase delay between the measured sea levels and the predicted tides from which the residuals were calculated. It was found that this phase delay in the tides could also be reproduced by the model, by combining atmospheric and tidal forcing in the model and subsequently removing a modelled 'tide-only' component. This result supports the idea that the enhanced westerly current during strong cold fronts interacts with the tidal current to displace the tidal node in Bass Strait to the east, resulting in a phase displacement. When tides that are predicted from phases and amplitudes determined from long tidal records, are then subtracted from the measured sea levels, a residual tidal signal

remains. This data processing procedure implicitly treats the oscillatory feature as part of the storm surge, however, model simulations in the present study that contain only atmospheric forcing, suggest that the storm-surge component would be more realistically represented in the data if the phase shift in the Bass Strait tides during strong westerly wind events was taken into account during data reduction. The results here also indicate that the model will be a useful tool in understanding the physical mechanism responsible for the phase delay in a subsequent study.

The role of atmospheric pressure forcing on the storm surge was investigated by conducting simulations with wind forcing only. It was found that the contribution to sea level due to pressure forcing was considerably less than that implied by an inverse barometer suggesting that atmospheric pressure forcing is not significant in these events and that the inverse barometer effect does not apply.

Model experiments were performed in which the western boundary of the computational domain was moved progressively eastwards to determine the influence of the upstream surge on the sea levels in Bass Strait. Results on all grids exhibited a reduction in sea-level heights with the most pronounced reduction occurring when the western boundary was located at the western entrance to Bass Strait. Here the reductions in storm-surge height were consistent with those predicted by analytical studies, although the reductions were not uniform and were more pronounced closer to the western boundary. The simulations indicated that the computational domain required to capture the sea level response in Bass Strait needed to cover much of the southern coastline.

Model simulations conducted to establish the relationship between changes in wind forcing and the resultant storm surge indicated that the relationship is linear with the change in sea level response being twice that of the change in wind speed. This high sensitivity to wind speed changes suggests that any variations in wind climatology due to enhanced greenhouse climate change could have a profound impact on the nature and frequency of surges along the south coast.

## Acknowledgments

The authors wish to express their gratitude to Mr Bill Mitchell and Drs Peter Baines, Geoff Lennon and John McBride who provided valuable discussions on aspects of the study. They are also grateful to the anonymous referees for their valuable comments and suggestions. The Bureau of Meteorology regional analyses were provided by Dr Paul Stewart. Dr

Harvey Stern (Bureau of Meteorology) and Mr Geoff Crapper (Melbourne Water) provided information on the 1934 flood event. The National Tidal Facility provided observational sea level data. The study was partially funded by EPA (Victoria) and Melbourne Water.

## References

- Adams, J.R. 1987. Tide levels during November - December 1934. Flood and high tide frequency analysis for Williamstown. *Board of Works Internal Report*, 64 pp.
- Baines, P.G., Hubbert, G.D. and Power, S. 1991. Fluid transport through Bass Strait. *Cont. Shelf Res.*, *11*, 269-93.
- Church, J.A. and Freeland, H.J. 1987. The energy source for the coastal-trapped waves in the Australian coastal experiment region. *J. Phys. Oceanogr.*, *17*, 289-300.
- Clarke, A.J. 1987. Origin of the coastally trapped waves observed during the Australian Coastal Experiment. *J. Phys. Oceanogr.*, *17*, 1847-59.
- Easton, A.K. 1970. The tides of the continent of Australia. Horace Lamb Centre, Flinders University, South Australia. *Research Paper No. 37*.
- Fandry, C.B., Hubbert, G.D. and McIntosh, P.C. 1985. Comparison of predictions of a numerical model and observations of tides in Bass Strait. *Aust. J. Mar. Freshw. Res.*, *36*, 737-52.
- Fandry, C. 1982. A numerical model of the wind-driven transient motion in Bass Strait. *J. geophys. Res.*, *87*, 489-517.
- Gill, A.E. 1982. *Atmosphere-Ocean Dynamics*. Academic Press, New York, 662 pp.
- Hubbert, G.D. and McInnes, K.L. 1999. A storm surge inundation model for coastal planning and impact studies. *J. Coastal Research*, *15*, 168-85.
- Hubbert, G.D., Leslie, L.M. and Manton, M.J. 1990. A storm surge model for the Australian region. *Q. Jl R. Met. Soc.*, *116*, 1005-20.
- Le Provost, C., Bennett, A.F. and Cartwright, D.E. 1995. Ocean tides for and from TOPEX/POSEIDON. *Science*, *267*, 639-42.
- McInnes, K.L. and Hess, D. 1992. Modifications to the Australian region limited area model and their impact on an east coast low event. *Aust. Met. Mag.*, *40*, 21-31.
- McInnes, K.L. and Hubbert, G.D. 2001. The impact of eastern Australian cut-off lows on coastal sea levels. *Meteorological Applications*, *8*, 229-43.
- McInnes, K.L., Hubbert, G.D., Abbs, D.J. and Oliver, S.E. 2002. A numerical modelling study of coastal flooding. *Meteorology and Atmospheric Physics*, *80*, 217-33.
- McInnes, K.L., McBride, J.L. and Leslie, L.M. 1994. Cold fronts over southeastern Australia: their representation in an operational numerical weather prediction model. *Weath. Forc.*, *9*, 384-409.
- Middleton, J.F. 1988. Long shelf waves generated by a coastal flux. *J. geophys. Res.*, *93*, 10,724-10,730.
- Middleton, J.F. and Viera, F. 1991. The forcing of low frequency motions in Bass Strait. *J. Phys. Oceanogr.*, *21*, 695-708.
- Middleton, J.F. 1991. Coastal-trapped wave scattering into and out of straits and bays. *J. Phys. Oceanogr.*, *21*, 681-694.
- Middleton, J.F. and Black, K.P. 1994. The low frequency circulation in and around Bass Strait: a numerical study. *Cont. Shelf Res.*, *14*, 1495-1521.
- Miller, M.J. and Thorpe, A.J. 1981. Radiation conditions for the lateral boundaries of limited-area numerical models. *Q. Jl R. Met. Soc.*, *107*, 615-28.
- Mills, G.A. and Seaman, R.S. 1990. The BMRC Regional Data Assimilation System. *Mon. Weath. Rev.*, *118*, 1217-37.
- Morrow, R.A., Stabeno, P.J., Smith, R.L. and Jones, I.S.F. 1990. Bass Strait forcing of coastal-trapped waves: ACE revisited. *J. Phys. Oceanogr.*, *20*, 1528-38.
- Provis, D.G. and Radok, R. 1979. Sea level oscillations along the Australian coast. *Aust. J. Mar. Freshw. Res.*, *30*, 295-301.
- Reeder, M.J., Keyser, D. and Schmidt, B.D. 1991. Three-dimensional baroclinic instability and summertime frontogenesis in the Australian region. *Q. Jl R. Met. Soc.*, *117*, 1-28.
- Signell, R.P. and Butman, B. 1992. Modelling tidal exchange and dispersion in Boston Harbour. *J. geophys. Res.*, *97*, 15591-606.
- Smith, S.D. and Banke, E.G. 1975. Variation of the sea surface drag coefficient with wind speed. *Q. Jl R. Met. Soc.*, *101*, 665-73.